AD-A234 745

Comparisons of Backscattering From Cylindrical Shells Described by Thin Shell and Elasticity Theories

A Paper Presented at the 120th Meeting of the Acoustical Society of America, November 1990, San Diego, California

Ronald P. Radlinski
Richard D. Vogelsong
Environmental & Tactical Support Systems Department

Louis R. Dragonette
Naval Research Laboratory

DTIC
ELECTE
APR 0 8 1991
C

Naval Underwater Systems Center
Newport, Rhode Island • New London, Connecticut

91 4 05 057

PREFACE

This document describes work performed under NUSC IR/IED Project A70204, *Scattering From Elastic Shells*, Principal Investigator R. P. Radlinski (Code 311), and under Code 31 Administrative Funds (631K11). The original sponsoring activity was the Navy Material Command (now the Space and Naval Warfare Systems Command), CAPT. Z. L. Newcomb (Code 05B).

REVIEWED AND APPROVED: 4 MARCH 1991

B. F. Cole

B. F. Cole
Head, Environmental & Tactical Support Systems Department

REPORT DOCUMENTATION PAGE

Public reporting burden for this collection of information is estimated to average 1 hour per response, including the time for reviewing instructions, searching existing data sources, gathering and maintaining the data needed, and completing and reviewing the collection of information. Send comments regarding this burden estimate or any other aspect of this collection of information, including suggestions for reducing this burden, to Washington Headquarters Services, Directorate for Information Operations and Reports, 1215 Jefferson Davis Highway, Suite 1204, Arlington, VA 22202-4302, and to the Office of Management and Budget, Paperwork Reduction Project (0704-0188), Washington, DC 20503

| 1. AGENCY USE ONLY (Leave blank) | 2. REPORT DATE
4 March 1991 | 3. REPORT TYPE AND DATES COVERED
Presentation |
|---|---|---|

4. TITLE AND SUBTITLE

Comparisons of Backscattering From Cylindrical Shells Described by Thin Shell and Elasticity Theories

5. FUNDING NUMBERS

ZN00001

6. AUTHOR(S)

Ronald P. Radlinski
Richard D. Vogelsong
Louis R. Dragonette (Naval Research Laboratory)

7. PERFORMING ORGANIZATION NAME(S) AND ADDRESS(ES)

Naval Underwater Systems Center
New London Laboratory
New London, Connecticut 06320

8. PERFORMING ORGANIZATION REPORT NUMBER

TD 8835

9. SPONSORING/MONITORING AGENCY NAME(S) AND ADDRESS(ES)

Naval Material Command (now SPAWAR)
Washington, DC 20363

10. SPONSORING/MONITORING AGENCY REPORT NUMBER

11. SUPPLEMENTARY NOTES

12a. DISTRIBUTION/AVAILABILITY STATEMENT

Approved for public release; distribution is unlimited.

12b. DISTRIBUTION CODE

13. ABSTRACT (Maximum 200 words)

For $kh \lesssim 0.65$, where k is the fluid wavenumber and h is the shell wall thickness, scattering from infinite cylindrical shells at normal incidence can be described by a combination of specular reflection and the zeroth order symmetric Lamb waves that correspond to extensional and inextensional modes of shell theory. Love-Timoshenko thin shell theory is found to closely describe the resonance scattering behavior from these types of structural modes. At higher values of kh, scattering from the antisymmetric Lamb-type flexural modes is predicted by full elasticity theory. For materials in which the plate and modified shear waves speeds can be either greater or less than the wave speed in the backscattering predictions of fluid, the accuracy of Love-Timoshenko thin shell theory will be investigated near the excitation of the antisymmetric Lamb-type flexural waves by comparisons with full elasticity theory. Plate theories will be used to develop a physical explanation of the resulting differences.

14. SUBJECT TERMS

Backscattering	Elasticity Theory	
Cylindrical Shell	Thin Shell Theory	

15. NUMBER OF PAGES
20

16. PRICE CODE

| 17. SECURITY CLASSIFICATION OF REPORT
UNCLASSIFIED | 18. SECURITY CLASSIFICATION OF THIS PAGE
UNCLASSIFIED | 19. SECURITY CLASSIFICATION OF ABSTRACT
UNCLASSIFIED | 20. LIMITATION OF ABSTRACT
SAR |
|---|---|---|---|

COMPARISONS OF BACKSCATTERING FROM CYLINDRICAL SHELLS DESCRIBED BY THIN SHELL AND ELASTICITY THEORIES

INTRODUCTION

The ability of thin shell theory to predict plane wave scattering from cylindrical shells has been recently discussed by Veksler and Korsunskii [J. Acoust. Soc. Am., 87, pp. 943–962 (1990)] for an iron shell. Both the plate wave speed and the modified shear wave speed of iron are greater than the wave speed of water. For a shell with an h/a of 1/64, where h is the wall thickness and a is the radius, the symmetric Lamb–type waves corresponding to extensional structural modes were closely predicted by Love–Timoshenko thin shell theory, but antisymmetric Lamb–type waves were not well predicted. In contrast, S. Baskar, V. V. Varadan, and V. K. Varadan [J. Acoust. Soc. Am., 75, pp. 1673–1679 (1984)] concluded that thin shell theory adequately predicted back-scattering in the range of excitation of antisymmetric Lamb–type waves for aluminum shells of h/a values of 0.15 for ka values up to 10.

For thin shell theory, zeroth order antisymmetric waves are predicted near the kh values of the coincidence frequency for the material. For materials where both the plate and shear wave speeds are greater than the sound speed in fluid, the deficiencies of thin shell theory in describing backscattering near the zeroth order antisymmetric Lamb wave response can be explained by analogies to plate theory. For materials with plate wave speeds greater than the wave speed in the fluid and with modified shear wave speeds less than the fluid wave speed, no zeroth order antisymmetric Lamb–type wave is predicted by either elasticity theory or thick shell theory. Accordingly, for this class of materials, thin shell theory predicts an antisymmetric Lamb–type wave that is of the wrong order.

1
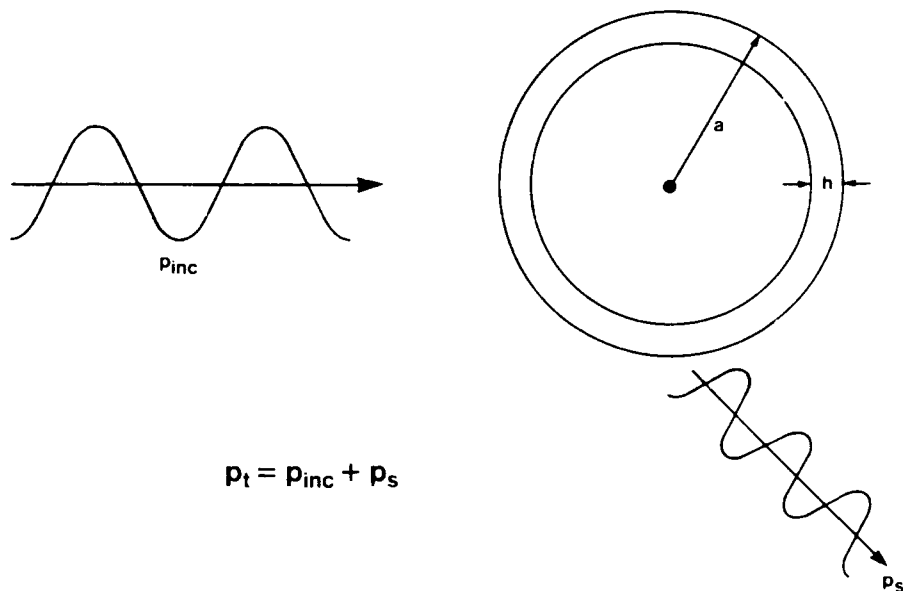
FIGURE 1

A plane wave is shown normally incident to an infinitely long cylindrical shell of wall thickness h and outer radius a. The total pressure p_t is given by the sum of the incident pressure p_{inc} and the scattered pressure p_s. The shell will be described by both elasticity theory and Love–Timoshenko thin shell theory. For elasticity theory, six boundary conditions must be satisfied, whereas for thin shell theory only three conditions need to be satisfied.

SCATTERING FROM AN ELASTIC CYLINDRICAL SHELL

$$p_{inc} = p_0 \sum_{n=0}^{\infty} \varepsilon_n i^n J_n(kr) \cos n\theta \qquad \varepsilon_n = \begin{matrix} 1 & n = 0 \\ 2 & n \neq 0 \end{matrix}$$

$$p_s(\theta) = -p_0 \sum_{n=0}^{\infty} \varepsilon_n i^n \left[\frac{J_n(ka) Q_n - ka J'_n(ka)}{H_n(ka) Q_n - ka H'_n(ka)} \right] H_n(kr) \cos n\theta$$

$$Q_n = \frac{\rho}{\rho_s} \frac{D_n^{(1)}(ka)}{D_n^{(2)}(ka)} = \frac{\rho}{\rho_s} \frac{\begin{vmatrix} a_{21} & a_{22} & a_{23} & a_{24} \\ a_{31} & a_{32} & a_{33} & a_{34} \\ a_{41} & a_{42} & a_{43} & a_{44} \\ a_{61} & a_{62} & a_{63} & a_{64} \end{vmatrix}}{\begin{vmatrix} a_{11} & a_{12} & a_{13} & a_{14} \\ a_{31} & a_{32} & a_{33} & a_{34} \\ a_{41} & a_{42} & a_{43} & a_{44} \\ a_{61} & a_{62} & a_{63} & a_{64} \end{vmatrix}} = \frac{i\omega a\rho}{Z_n}$$

FAR FIELD FORM FUNCTION $\qquad f_\infty(\theta) = \left[\frac{2r}{a} \right]^{1/2} \left| \frac{p_s(\theta)}{p_{inc}} \right|$

FIGURE 2

In the formulation of scattering by elasticity theory, the incident and scattered pressures are expressed in cylindrical harmonics [J. J. Faran, J. Acoust. Soc. Am., 23, pp. 405–418 (1951)]. Both shear and dilatational waves describe the motion within the shell. Three boundary conditions must be satisfied at both the inner and outer radii. The boundary conditions are as follows: (1) the normal stress in the shell equals the negative of the total pressure in the fluid, (2) the normal velocity in the shell is proportional to the normal derivative of the total pressure, and (3) the tangential stress is zero on the boundary of the cylinder.

The function Q_n defines the shell elasticity. Here ρ_s is the density of the shell and ρ is the density of the fluid. Q_n also is shown to be related to the modal impedance Z_n, where $Z_n = (\dot{p}_t)_n / \dot{W}_n$, with $\dot{W}_n$ being the normal modal velocity of the elastic shell. With this definition, the scattered pressure p_s can be written by an expression that is consistent with shell theory, as shown in the next figure. Resonance scattering occurs in the scattered pressure p_s at ka values where the determinant in the denominator of the expression for Q_n is zero or, equivalently, where the modal impedance Z_n is zero. The backscattered pressure will be expressed in terms of the farfield form function f_∞.

LOVE - TIMOSHENKO THIN SHELL EQUATIONS

$$\varrho_s h \omega^2 W - \frac{Eh}{a^2(1-v^2)}\left(\frac{dV}{d\theta}+W\right) - \frac{Eh^3}{12a^4(1-v^2)}\frac{d^3}{d\theta^3}\left(\frac{dW}{d\theta}-V\right) = p_t$$

$$\varrho_s h \omega^2 V + \frac{Eh}{a^2(1-v^2)}\frac{d}{d\theta}\left(\frac{dV}{d\theta}+W\right) - \frac{Eh^3}{12a^4(1-v^2)}\frac{d^2}{d\theta^2}\left(\frac{dW}{d\theta}-V\right) = 0$$

$$W = \sum_0^\infty W_n \cos(n\theta) \qquad V = \sum_0^\infty V_n \sin(n\theta)$$

$$P_t = -i\omega \sum_{n=0}^\infty Z_n W_n \cos(n\theta)$$

$$P_s(\theta) = -p_0 \sum_{n=0}^\infty \varepsilon_n i^n \left\{\frac{\rho c\, J_n(ka) + iJ'_n(ka)\, Z_n}{\rho c\, H_n(ka) + iH'_n(ka)\, Z_n}\right\} H_n(kr) \cos n\theta$$

$$Z_n = i\rho_s h\omega \left\{1 - \frac{E}{\rho_s\omega^2 a^2(1-v^2)}\left[1 + n^4/12(h/a)^2 + \frac{n^2[1 + (n^2/12)(h/a)^2]^2}{\omega^2 a^2 \varrho_s(1-v^2)/E - n^2[1+(h/a)^2/12]}\right]\right\}$$

FIGURE 3

The normal and tangential stress equations that describe Love–Timoshenko thin shell theory include (1) an inertial term, (2) a term that describes extensional motion, and (3) a term that describes inextensional motion. The first equation represents the normal stress at the midsurface of the shell, which is equal to the negative of the total pressure in the fluid. The second equation represents the tangential stress, which is zero at the fluid interface. W and V, the normal and tangential displacements, respectively, are expanded in terms of the circular functions. When V is eliminated from the stress equations, the total pressure can be written in terms of a sum of modal impedances Z_n times the normal modal velocities ($-i\omega W_n$). The additional boundary condition is that the normal velocity at the midsurface of the shell is proportional to the normal derivative of the total pressure. The scattered pressure p_s can then be written in terms of the modal impedance Z_n. In the expression for the modal impedance, E is Young's modulus and v is Poisson's ratio. For a cylindrical shell, the Love–Timoshenko equations are equivalent to those developed by Junger ["Sound Scattering by Thin Elastic Shells," J. Acoust. Soc. Am., 24, pp. 365–373 (1952)].

RESONANCE FREQUENCIES FOR AN INFINITE CYLINDRICAL SHELL

(EXTENSIONAL)

$\frac{\omega^{(2)}a}{c_p}$

h/a = 0.05

h/a = 0.025

$\frac{\omega a}{c_p}$

10

1

0.1

$\frac{\omega^{(1)}a}{c_p}$

(INEXTENSIONAL)

0 2 4 6 8 10 12 14 16 18 20 22 24
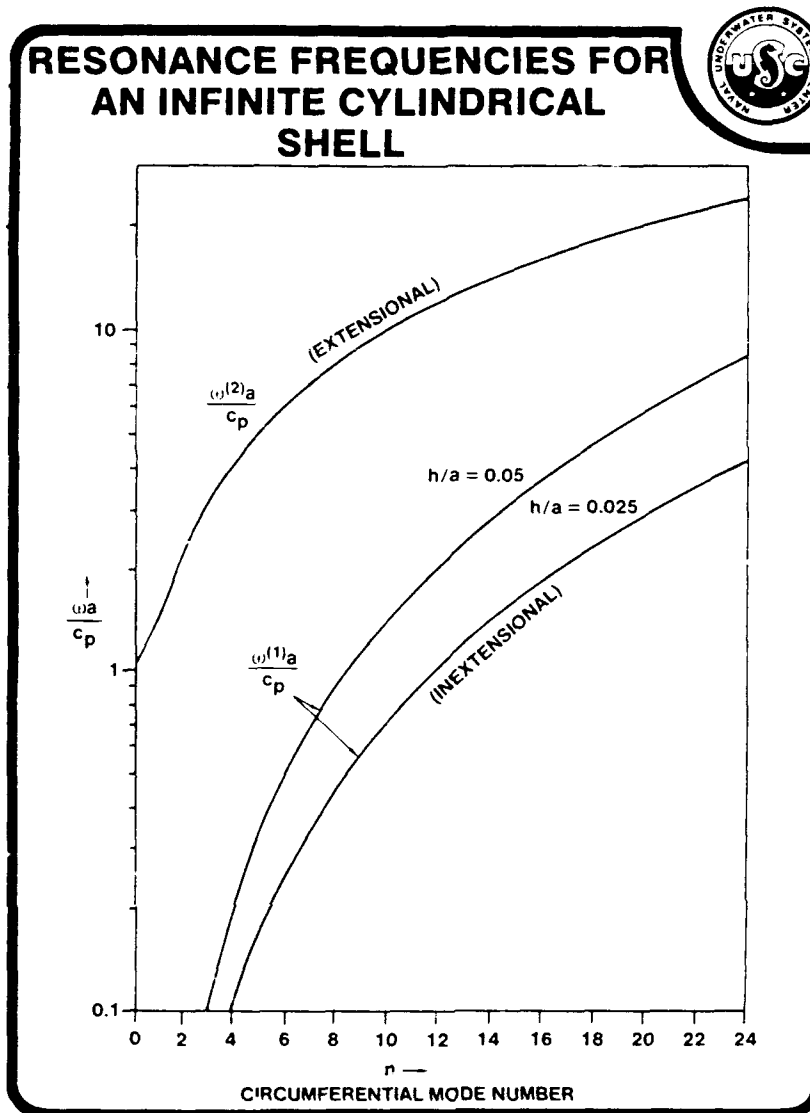
n —

CIRCUMFERENTIAL MODE NUMBER

FIGURE 4

The resonance frequencies calculated from the shell theory shown here as a function of circumferential mode number are from Junger and Feit [Sound, Structures, and Their Interaction, MIT Press, Cambridge, MA (1986)]. The discrete modes are shown as continuous functions. The term c_p along the ordinate axis is the plate velocity of the shell material. Note that there are two solutions to the eigenfrequency equation for the resonance frequencies of the shell. The inextensional modes, which start at lower frequencies, depend on the shell thickness. The extensional modes are essentially independent of wall thickness.

ARMCO IRON SHELL
(Veksler & Korsunskii) h=a/64
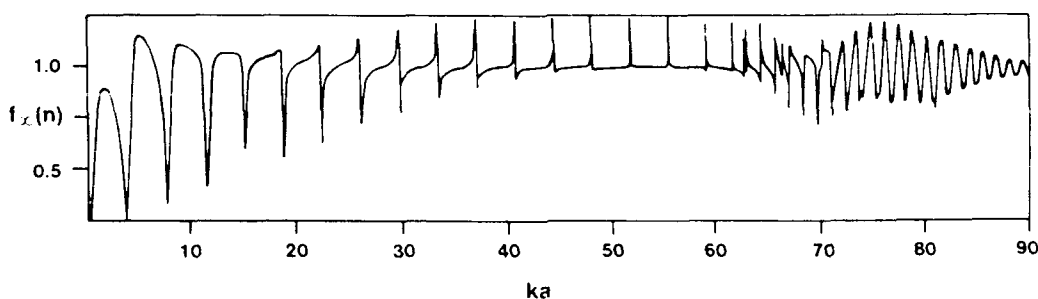## ELASTICITY THEORY

ka
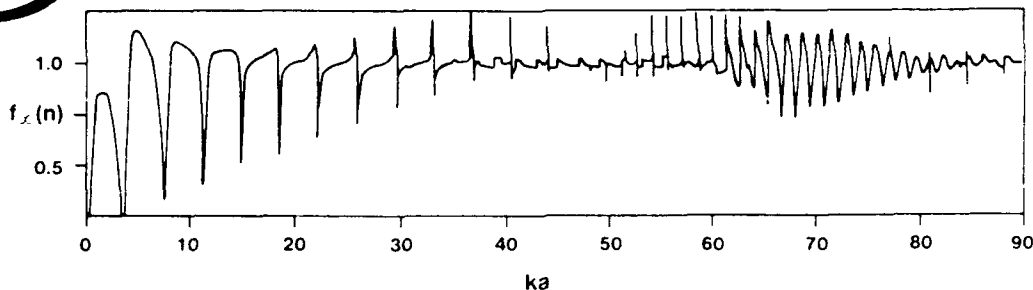
LOVE – TIMOSHENKO SHELL THEORY

ka

FIGURE 5

A comparison of the backscattered form function from a shell with h/a of 1/64 as calculated by thin shell theory and full elasticity theory is shown from the paper by Veksler and Korsunskii. Below a ka value of 30, no differences are seen in the two theories. At low ka, the form function is described by the interaction of the specular reflection, which experiences a 180° phase change at the acoustical soft cylinder, with the extensional modes or symmetric Lamb–type waves that circumnavigate the cylinder. The destructive interference of the out–of–phase waves results in nulls in the form function. With increased ka, the cylinder begins to look more rigid to the incident wave; thus, the specular and the creeping waves begin to combine constructively to form narrow peaks in the form function.

Above a ka value of 30, elasticity theory predicts additional structure, which is not seen in Veksler's calculation for a thin shell. Redoing Veksler's thin shell theory calculations with increased ka resolution results in narrow bandwidth bending resonances, which fall between the extensional modes. For materials in which both the plate and

shear wave speeds are greater than for the fluid, Dragonette [NRL Report No. 8216, Naval Research Laboratory (1978)] has indicated a correspondence of excitation of flexural Lamb waves with the coincidence frequency for plates. At the coincidence frequency, the wave speed in the shell equals the wave speed in the fluid. Above a ka value of 60, which corresponds to the coincidence frequency for a flat plate of the same thickness as the shell, poor agreement is seen in the two solutions for the predictions of the antisymmetric Lamb-type waves. Veksler and Korsunskii concluded that the antisymmetric waves are not well predicted by Love-Timoshenko thin shell theory. The basis of this poor agreement will be discussed later.
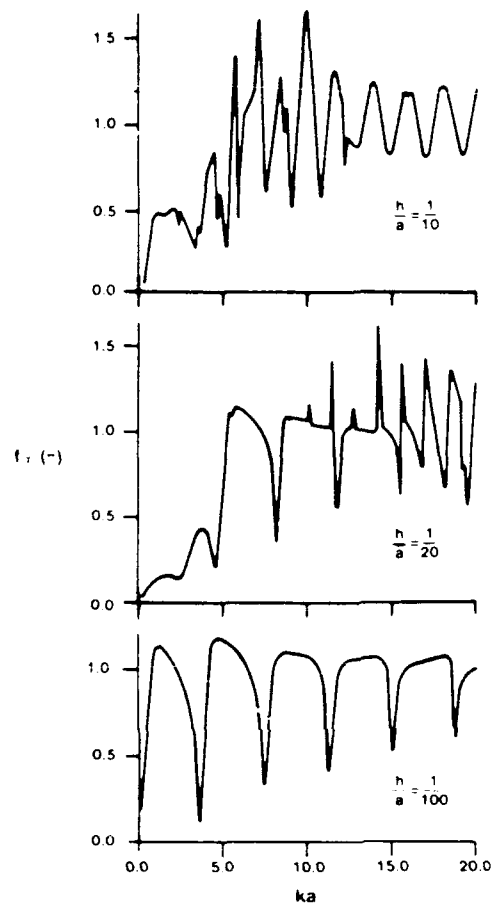
FIGURE 6

The backscattered form function as calculated from elasticity theory is shown as a function of ka for steel shells of increasing shell thickness. For a shell of wall thickness to radius ratio (h/a) of 1/100, the form function is described by the interaction of the specular reflection with the symmetric extensional modes. For h/a of 1/20 shell, the antisymmetric Lamb-type flexural wave appears above a ka of 15. The slower phase velocity of this wave causes more rapid fluctuations in the form function. Between a ka of 5 to 15, the narrow peaks are due to the inextensional bending modes. For h/a of 1/10, the antisymmetric flexural waves and the symmetric bending waves interact with the extensional resonances at even lower values of ka.
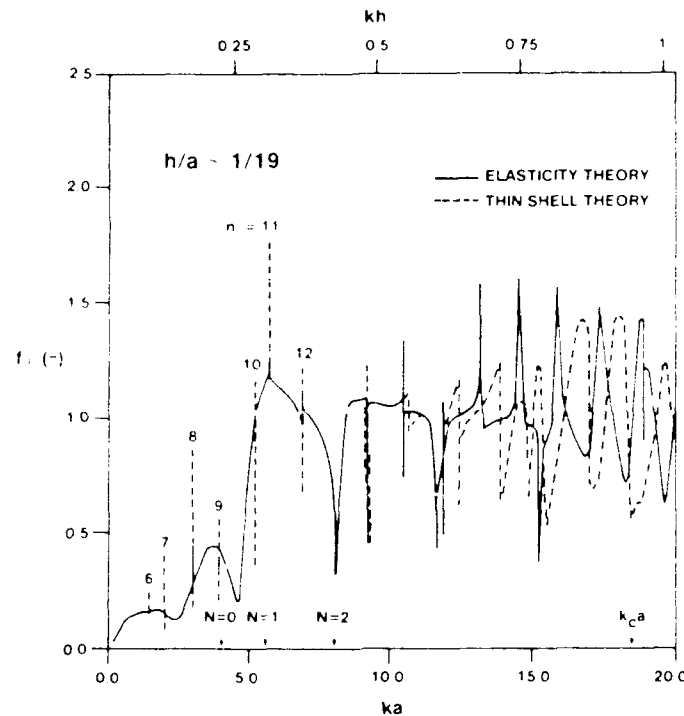
BACKSCATTERING FROM A STEEL SHELL

FIGURE 7

A comparison of elasticity theory with Love-Timoshenko thin shell theory for a steel shell of h/a value of 1/19 is plotted for ka values along the abscissa and kh along the top of the graph. In this example, the three different modes discussed in the previous figure can be separately identified. The first three in-air extensional mode numbers are designated on the abscissa by N. At ka values below 10, good agreement is found between the two theories. Narrow resonances due to bending modes designated by n' begin to appear at a modal number of six. At low values of ka, the wavelength of the incident wave is too large to distinguish these non-net volume velocity bending modes. Differences between the shell theory and elasticity theory in prediction of the narrow bending modes are due to the higher ka resolution of the shell theory calculations. The asymmetric Lamb-type waves due to flexure are predicted by thin shell theory above a ka of 12, but the agreement with full elasticity theory is poor. Note that coincidence frequency for a plate of the same thickness as the shell is predicted at a ka value of about 18. Plate theory results will now be used to investigate the shortcomings of thin shell theory.

PLATE THEORIES

THIN PLATES	THICK PLATES

COINCIDENCE FREQUENCY

$$\omega_c = \frac{\sqrt{12}}{h} \frac{c^2}{c_p}$$

$$\omega_{TM}^2 = \frac{\omega_c^2}{\left(1 - \frac{c^2}{c_p^2}\right)\left(1 - \frac{c^2}{c_s^2}\right)}$$

COINCIDENCE ANGLE

$$\cos^2\theta_c = \frac{\omega_c}{\omega}$$

$$\cos^2\theta_{TM} = \frac{1}{2}\left[\left(\frac{c}{c_s}\right)^2 + \left(\frac{c}{c_p}\right)^2 \pm \sqrt{\left[\left(\frac{c}{c_s}\right)^2 - \left(\frac{c}{c_p}\right)^2\right]^2 + 4\left(\frac{\omega_c}{\omega}\right)^2}\right]$$

MODIFIED SHEAR VELOCITY

$$c_s = \kappa\left(\frac{\mu}{\rho_s}\right)^{1/2} \qquad \kappa = \left[\frac{0.87 + 1.12\nu}{1 + \nu}\right]$$

THIN PLATE THEORY VALID FOR

$$\omega < \left[0.1\left(\frac{\pi}{\sqrt{12}}\right)\frac{c_s c_p}{c^2}\right]\omega_c$$

PLATE WAVE VELOCITY

$$c_p = \sqrt{\frac{E}{\rho_s(1 - \nu^2)}}$$

μ = SHEAR MODULUS
E = YOUNG'S MODULUS
ν = POISSON'S RATIO
ρ_s = MATERIAL DENSITY

FLUID VELOCITY c

FIGURE 8

The coincidence frequency for classical thin plate theory only depends on (1) the plate velocity c_p, (2) the wave speed in the fluid that is designated by c, and (3) the plate thickness. The coincidence frequency for thick plate theory is a function of both the plate velocity and the modified shear velocity c_s. If $c_s < c < c_p$ or $c_p < c < c_s$, no coincidence frequency is predicted. Also for $c_s, c_p > c$, two coincident angles are predicted by thick plate theory. Mindlin [J. Applied Mechanics, 18, pp. 31-38 (1951)] has shown that to a first approximation the validity of thin plate theory is dependent on the ratios of the modified shear and plate velocities to that of the fluid wave speed. As the values of the modified shear and plate velocities decrease, thin shell theory is expected to be a poorer approximation to the generation of antisymmetric Lamb-type flexural waves.
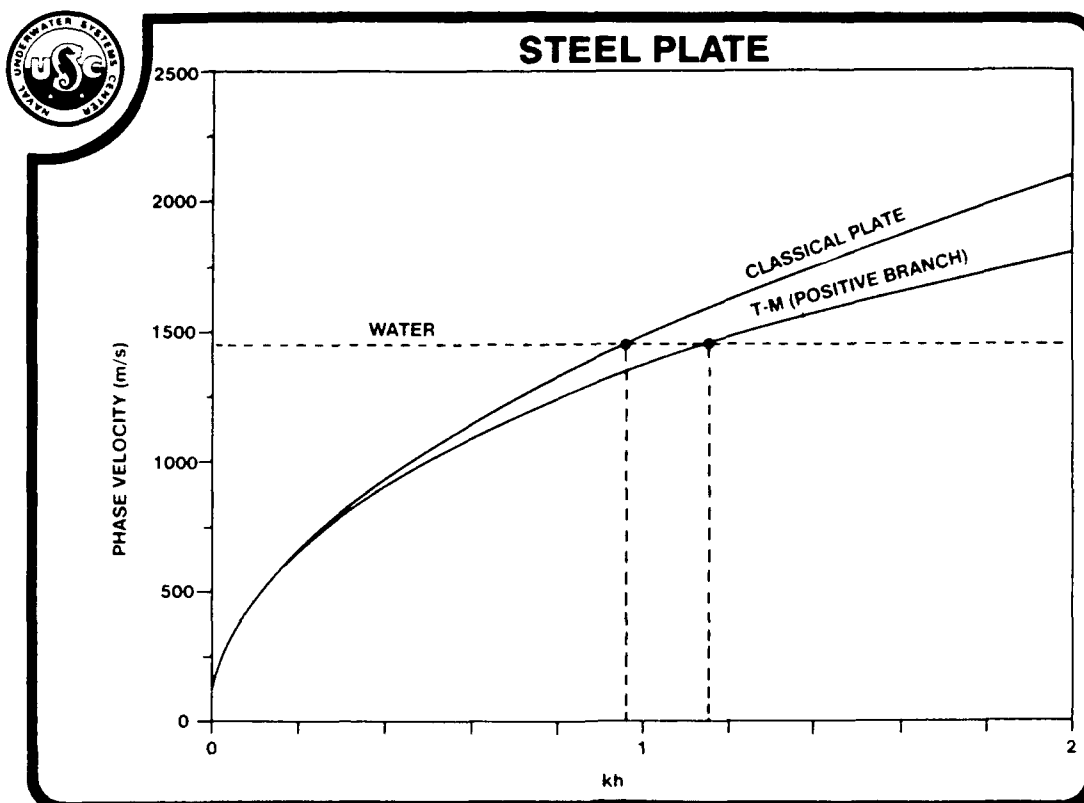
STEEL PLATE

FIGURE 9

A plot of the phase velocity of a steel plate as a function of kh indicates that for classical plate theory the coincidence frequency is predicted to occur at a lower value of kh than for the positive branch of the Timoshenko–Mindlin thick plate theory. Thus, classical plate theory will yield errors in the prediction of the antisymmetric Lamb–type flexural waves at lower values of ka than will the Timoshenko–Mindlin plate theory. This will be true for all materials in which both the modified shear wave speed and the plate wave speed are greater than the wave speed in the fluid.
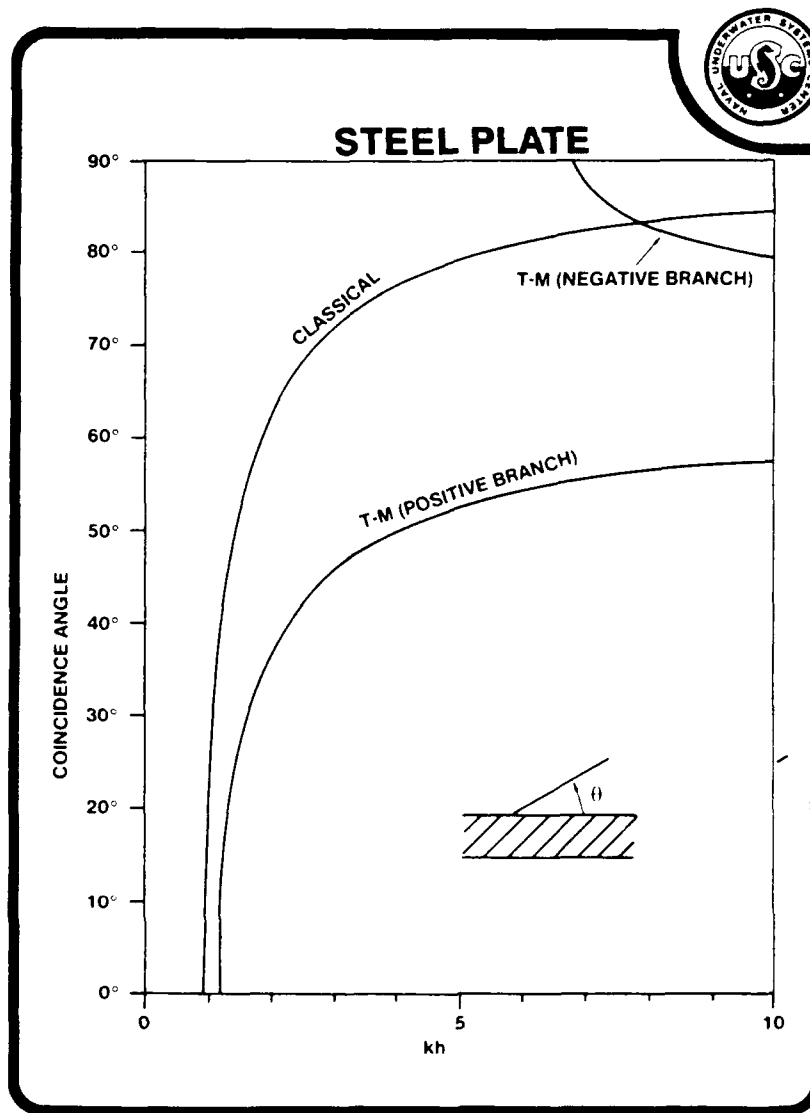
FIGURE 10

The coincidence angle is shown as a function of kh for classical plate theory and Timoshenko–Mindlin thick plate theory. The coincidence angle is defined as a grazing angle with respect to the plate. Corresponding to the phase velocity predictions, the classical coincidence angle is typically greater than is the angle for the positive branch of thick plate theory and begins at a lower value of kh. Note that the second coincidence angle for the negative branch of the thick plate theory is predicted at higher values of kh and begins at normal incidence, or 90°, with respect to the plate.

BACKSCATTERING FROM LEXAN
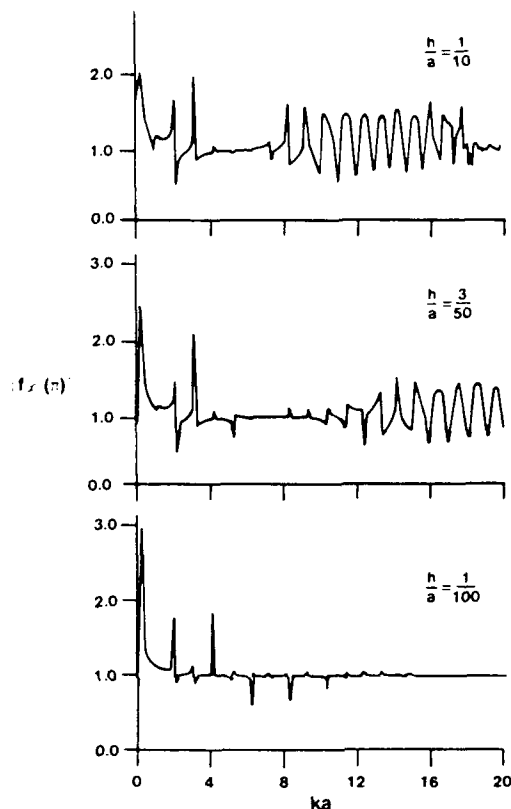PLASTIC SHELLS OF VARIOUS
THICKNESS (ELASTICITY THEORY)

FIGURE 11

The backscattered form function as calculated by elasticity theory is shown as a function of ka for plastic shells of increasing shell thickness. The low ka behavior of the plastic shell is different from the iron and steel shells because of the much lower plate and modified shear velocities of plastic. The first peak in all three curves is due to the $N=0$ extensional mode of the shell. For the plastic material with a smaller impedance mismatch with respect to the fluid, there is no evidence of additional narrow resonances due to symmetric bending modes. Again, as the thickness of the shell increases, the antisymmetric Lamb–type waves appear at lower values of ka. It will now be shown that the generation of the antisymmetric Lamb–type flexural waves has a different character than was seen for the steel shell.

13

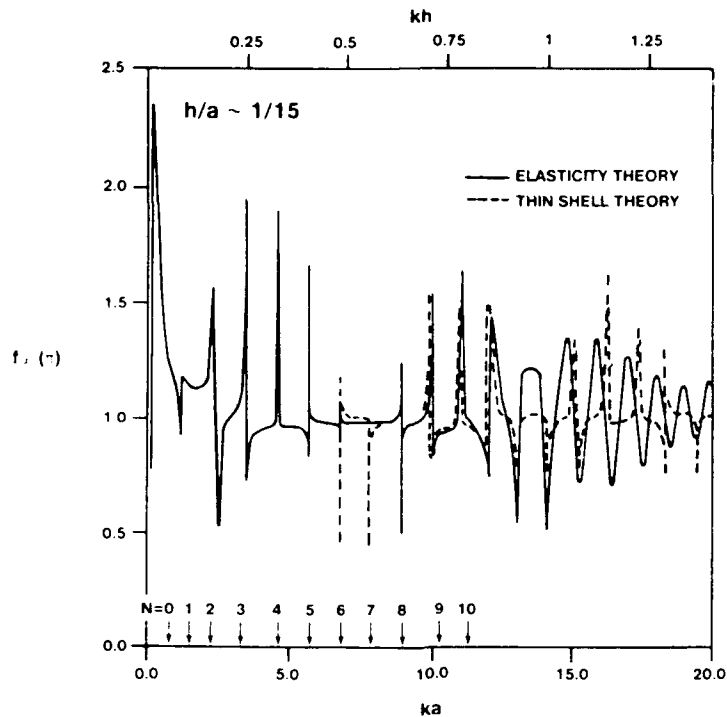FIGURE 12

A comparison between shell theory and elasticity theory is shown for a plastic shell with an h/a value of 1/15. Both ka and kh horizontal axes are shown. The ka values for the first 10 in-air extensional modes are shown along the lower abscissa. The plastic has a plate wave speed greater than water but a modified shear wave speed less than the wave speed for the fluid. The first resonance can be predicted by accounting for the fluid loading on the N=0 extensional mode. For ka values less than 12, the form function predicted by thin shell theory compares well with that predicted by elasticity theory. Above a ka of 12, elasticity theory predicts an antisymmetric Lamb-type flexural wave, but the thin shell theory continues to only predict the narrow symmetric extensional Lamb-type wave. Note that the maximum value of kh on this plot is about 1.5.
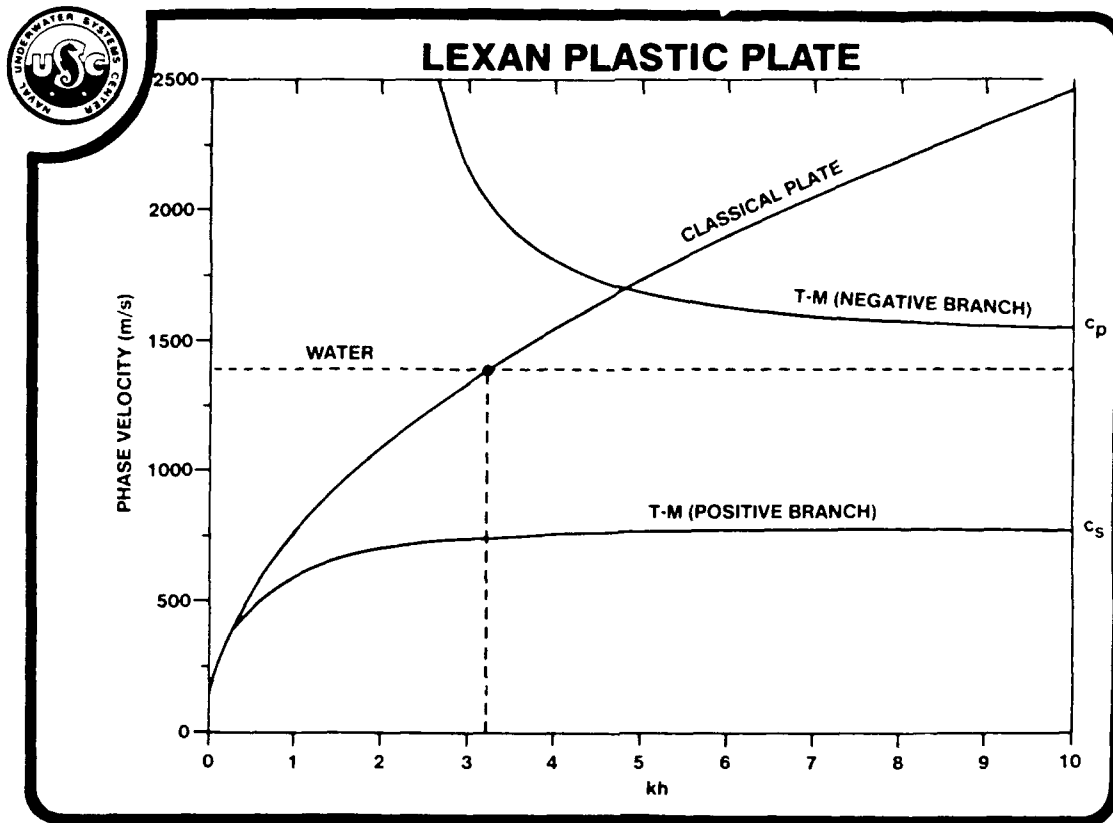
LEXAN PLASTIC PLATE

FIGURE 13

The phase velocity for a plastic plate is plotted versus kh. The coincidence angle predicted by classical plate theory is above a kh value of 3. No coincidence frequency is predicted for the phase velocity of the positive branch of the Timoshenko–Mindlin theory, which asymptotes at the modified shear wave speed c_s. The second flexural branch has a phase velocity that is greater than wave speed for the fluid.
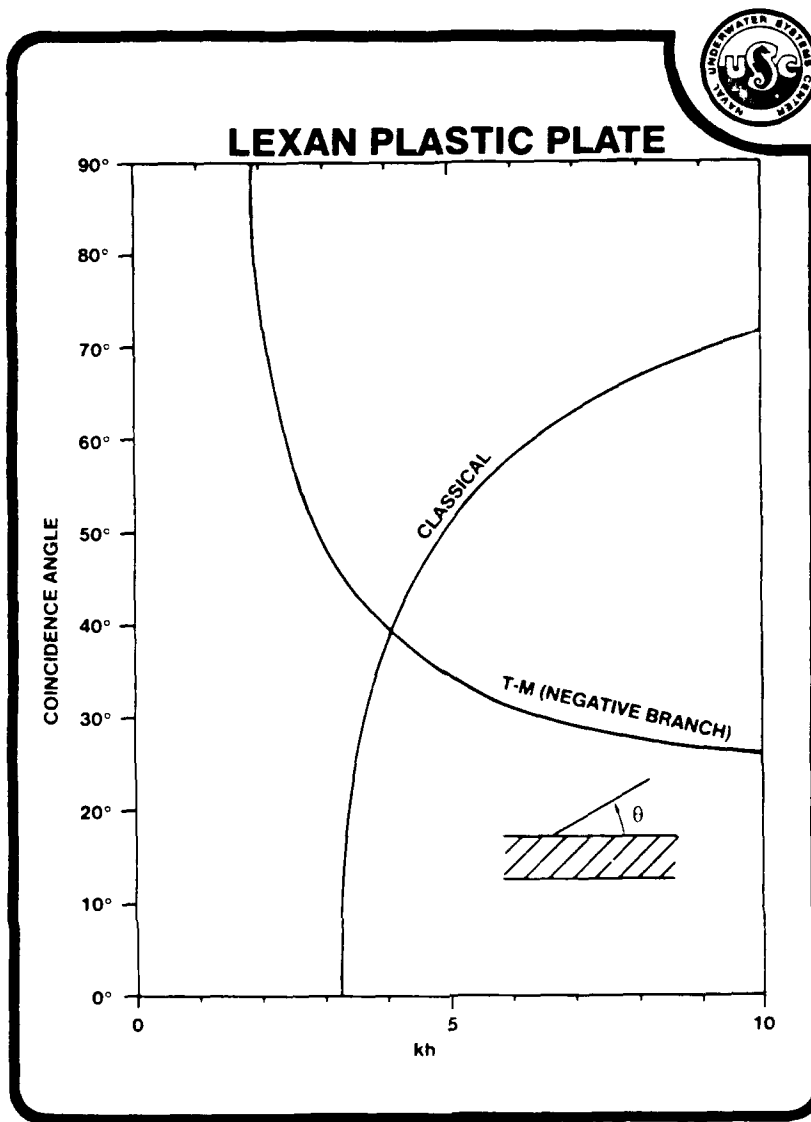
FIGURE 14

The predicted coincidence angles for a plastic plate are plotted as a function of kh for both classical and thick plate theory. Below a kh value of 2, the second branch of the thick plate theory predicts a coincidence angle near 90° (normal to the plate). Classical plate theory does not predict a coincidence angle until just above a kh value of 3, where coincidence is predicted to occur at the grazing angle of zero degrees. The antisymmetric Lamb-type wave predicted by shell elasticity theory in figure 12 is due to the second antisymmetric flexural Lamb-type wave. Thin shell theory fails to predict this type of flexural wave.

LEAD PLATE

$c_s, c_p < c$

CLASSICAL

WATER

T-M (NEGATIVE BRANCH)

c_p

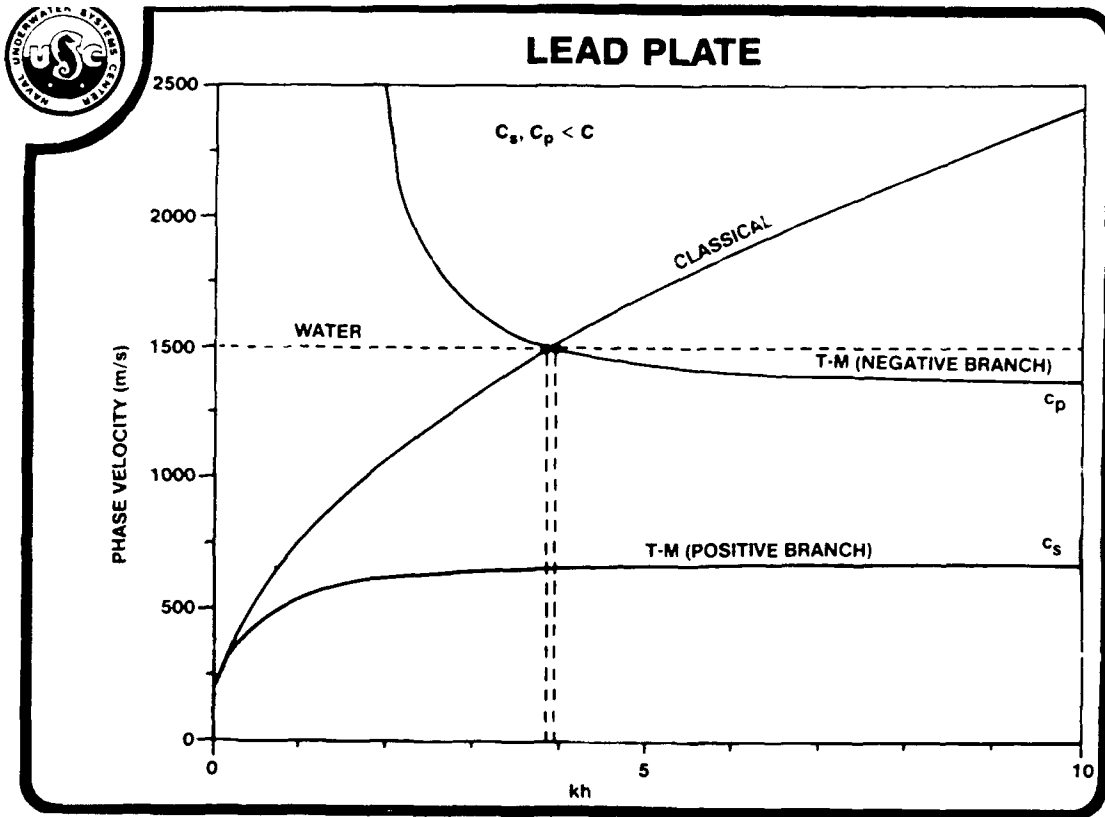T-M (POSITIVE BRANCH)

c_s

PHASE VELOCITY (m/s)

kh

FIGURE 15

For a material such as lead for which both the modified shear velocity and the plate velocity are less than water, the classical coincidence frequency for the negative branch is close to that predicted by the classical plate theory. Note that the asymptotic behavior of the negative branch approaches c_p, which is less than the wave speed in water.
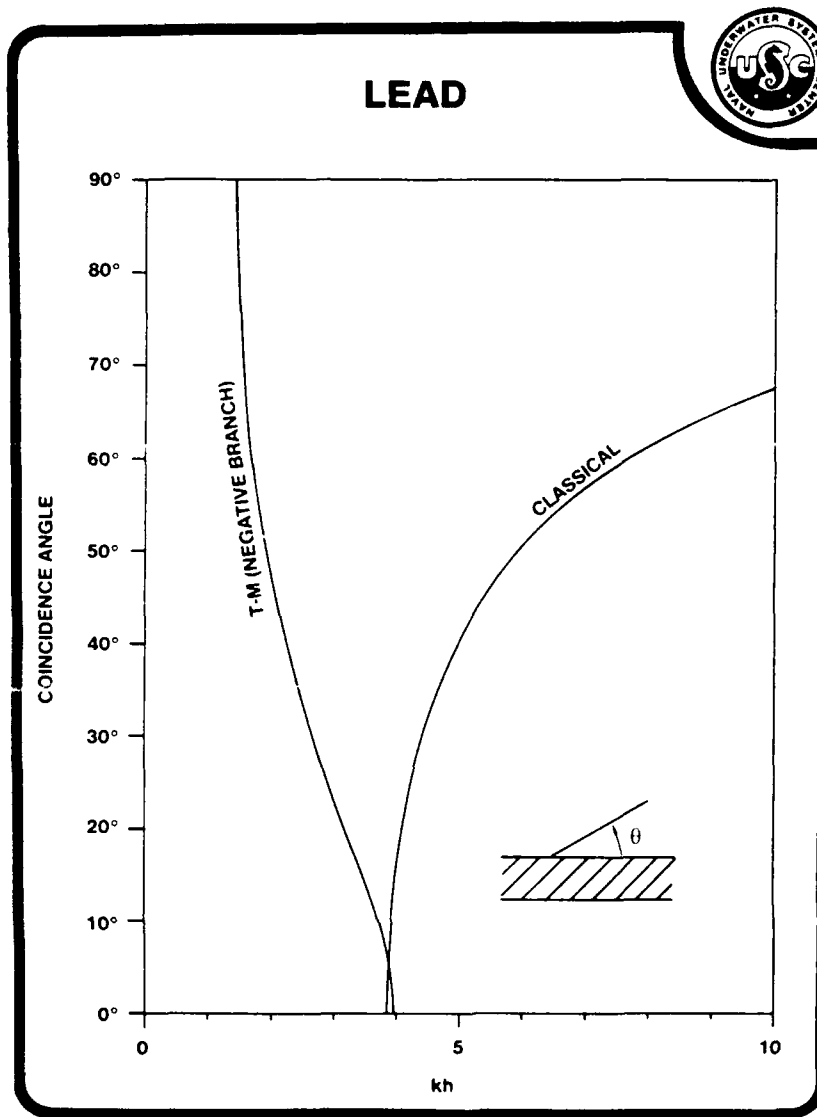
FIGURE 16

The coincidence angles predicted for lead by thick plate theory are associated with the second branch and begin at 90° (normal to the plate). As with the plastic plate, the coincidence effect begins at kh values much lower than that associated with the coincidence frequency. Thus, the antisymmetric Lamb-type waves predicted by thick plate theory and elastic shell theory would be much lower than those predicted by classical thin shell theory.

CONCLUSIONS

At low values of kh, the interaction of the specular-reflected waves and the extensional modes described by thin shell theory agrees well with the scattering from shells predicted by full elasticity theory. Because the inextensional symmetric modes have no net volume velocity for a circular cylindrical shell, they contribute as narrow resonances at intermediate values of kh where the bending motion can be distinguished at the smaller wavelengths.

The analysis confirms that the validity of thin shell theory predictions for the antisymmetric flexural resonances is directly proportional to the ratio of the modified shear wave speed and the ratio of plate wave speed to that of the wave speed of the fluid. For materials where either or both the plate and shear wave speeds are less than that for fluid, the generation of the second order antisymmetric wave has no correspondence to the classical coincidence frequency. In general, to accurately predict backscattering by the lower order antisymmetric Lamb-type flexural waves predicted by full elasticity theory, a thick shell theory must be employed.

CONCLUSIONS

- THIN SHELL THEORY ACCURATELY PREDICTS SPECULAR/ SYMMETRIC LAMB-TYPE WAVE INTERACTION

- ACCURACY OF THIN SHELL THEORY PREDICTION OF ANTISYMMETRIC LAMB-TYPE WAVES IS MATERIAL DEPENDENT

- FOR c_p, c_s > c, ANTISYMMETRIC WAVES FOR THIN SHELL THEORY PREDICTED AT LOWER ka THAN ELASTICITY THEORY OR THICK SHELL THEORY

- FOR c_p > c > c_s ANTISYMMETRIC WAVES FOR THIN SHELL THEORY PREDICTED AT HIGHER ka THAN ELASTICITY THEORY

- FOR c > c_p, c_s ANTISYMMETRIC WAVES FOR THIN SHELL THEORY PREDICTED AT MUCH HIGHER ka THAN ELASTICITY THEORY

- THICK SHELL THEORY NEEDED TO ACCURATELY PREDICT ANTISYMMETRIC LAMB-TYPE WAVE SCATTERING

FIGURE 17

INITIAL DISTRIBUTION LIST

Addressee	No. of Copies
NRL, Washington, DC (L. Dragonette, D. Photiadis, J. Bucaro, L. Schuetz, C. Gaumond, D. Bradley)	6
DTRC, Bethesda, MD (J. Niemiec, W. Blake, M. Rumerman D. Feit, S. McKeon)	5
DTIC	12
Washington State University (Philip Marston)	1
NOARL, Stennis Space Center (M. Werby, C. Dean)	2
NSWC, White Oak (G. Gaunaurd)	1
NOSC (H. Schenck)	1
Pennsylvania State University (A. Pierce, V. K. Varadan, S. Hayek, C. Burroughs)	4
Orincon (J. Young)	1
Alliant Techsystems, Inc. (M. M. Simon)	1
ONR, Arlington (A. Tucker (Code 122), G. Main (Code 1222), P. Abraham (Code 1132))	3
University of Rhode Island (P. Stephanisen)	1
Atlantic Applied Research Corp. (P. H. White)	1
Georgia Institute of Technology (J. Ginsberg)	1
Cambridge Acoustical Associates (J. Garralick)	1